



On-chip spectroscopy with thermally tuned high-Q photonic crystal cavities

Andreas C. Liapis, Boshen Gao, Mahmudur R. Siddiqui, Zhimin Shi, and Robert W. Boyd

Citation: [Applied Physics Letters](#) **108**, 021105 (2016); doi: 10.1063/1.4939659

View online: <http://dx.doi.org/10.1063/1.4939659>

View Table of Contents: <http://scitation.aip.org/content/aip/journal/apl/108/2?ver=pdfcov>

Published by the [AIP Publishing](#)

Articles you may be interested in

[High sensitivity and high Q-factor nanoslotted parallel quadrabeam photonic crystal cavity for real-time and label-free sensing](#)

Appl. Phys. Lett. **105**, 063118 (2014); 10.1063/1.4867254

[High sensitivity gas sensor based on high-Q suspended polymer photonic crystal nanocavity](#)

Appl. Phys. Lett. **104**, 241108 (2014); 10.1063/1.4879735

[Photonic crystal slot waveguide absorption spectrometer for on-chip near-infrared spectroscopy of xylene in water](#)

Appl. Phys. Lett. **98**, 023304 (2011); 10.1063/1.3531560

[Measurements of total peroxy and alkyl nitrate abundances in laboratory-generated gas samples by thermal dissociation cavity ring-down spectroscopy](#)

Rev. Sci. Instrum. **80**, 114101 (2009); 10.1063/1.3258204

[APL Photonics](#)

The advertisement features a blue background with a molecular structure graphic. On the left is a thumbnail of an 'Applied Physics Reviews' journal cover. The main text reads 'NEW Special Topic Sections' in large white letters. Below this, it says 'NOW ONLINE' in yellow, followed by 'Lithium Niobate Properties and Applications: Reviews of Emerging Trends' in white. The AIP Applied Physics Reviews logo is in the bottom right corner.

NEW Special Topic Sections

NOW ONLINE
Lithium Niobate Properties and Applications:
Reviews of Emerging Trends

AIP Applied Physics Reviews

On-chip spectroscopy with thermally tuned high-Q photonic crystal cavities

Andreas C. Liapis,^{1,a),b)} Boshen Gao,^{1,b)} Mahmudur R. Siddiqui,¹ Zhimin Shi,²
 and Robert W. Boyd^{1,3}

¹The Institute of Optics, University of Rochester, Rochester, New York 14627, USA

²Department of Physics, University of South Florida, Tampa, Florida 33620, USA

³Department of Physics and School of Electrical Engineering and Computer Science, University of Ottawa, Ottawa, Ontario K1N 6N5, Canada

(Received 3 November 2015; accepted 26 December 2015; published online 11 January 2016)

Spectroscopic methods are a sensitive way to determine the chemical composition of potentially hazardous materials. Here, we demonstrate that thermally tuned high-Q photonic crystal cavities can be used as a compact high-resolution on-chip spectrometer. We have used such a chip-scale spectrometer to measure the absorption spectra of both acetylene and hydrogen cyanide in the 1550 nm spectral band and show that we can discriminate between the two chemical species even though the two materials have spectral features in the same spectral region. Our results pave the way for the development of chip-size chemical sensors that can detect toxic substances. © 2016 AIP Publishing LLC. [<http://dx.doi.org/10.1063/1.4939659>]

The past decade has seen a marked increase in the demand for compact, integrated devices that can reliably identify chemical and biological agents. Miniaturized spectrometers, in particular, have received much attention. Broadly speaking, two categories of on-chip spectrometers exist: First, there are dispersive spectrometers, such as arrayed-waveguide grating (AWG) spectrometers,^{1,2} super-prism spectrometers,^{3,4} grating-based spectrometers,^{5,6} and on-chip implementations of the Mach-Zehnder geometry.⁷ However, these devices tend to be rather large, with a resolution in wavenumbers (cm^{-1}) typically given by $1/L$, where L is the characteristic size of the dispersive region in cm. Spectrometers can also be constructed by cascading optical elements with narrow-band spectral responses such as Fabry-Pérot filters,⁸ grating couplers,⁹ microdonut resonators,¹⁰ and photonic crystal (PhC) cavities.^{11–13} The operating principle of such a spectrometer is shown schematically in Fig. 1(a) and can be described as follows.

The spectrum to be measured is injected into a bus waveguide that is coupled to a number of resonators, each tuned to a different wavelength. The light scattered by each resonator, either vertically, as in Gan *et al.*,¹² or into output waveguides, as in Xia *et al.*,¹⁰ is monitored and used to reconstruct the input spectrum. The resolution of such a spectrometer is given by the spectral width of the frequency response of the individual elements, which is typically of the order of 10 GHz. Conversely, the total number of resolvable spectral lines, that is, the number of resonators that can be used, is limited by their free spectral range, that is, the separation between adjacent resonance frequencies of the cavity. Note that, in practice, the total number of resonators is limited by the loss introduced by each element for the non-resonant frequency component. The drawback of cascaded spectrometers is that they require additional optics to couple light into and out of the resonators, which increases the device size and complicates its operation.

In this letter, we demonstrate high-resolution spectroscopy based on a single tunable high-Q silicon PhC cavity that both emits into and is excited from the vertical direction, thus eliminating the need for a bus waveguide entirely [Fig. 1(b)]. In addition, we demonstrate that such a cavity can readily be used to discriminate between the absorption spectra of different chemical species. Two gases are considered here, acetylene ($^{12}\text{C}_2\text{H}_2$) and hydrogen cyanide (H^{12}CN). These are commonly used as wavelength references, with strong absorption lines in the vicinity of 1530 nm. Both gases are used industrially, but hydrogen cyanide is highly toxic. Our results therefore pave the way for the development of chip-size chemical sensors that can detect the presence of toxic substances.

We have fabricated PhC cavities with enhanced vertical coupling using a design protocol similar to that of Tran *et al.*¹⁴ These cavities consist of a triangular lattice of air holes on a thin silicon membrane, with three holes omitted, forming an L-3 cavity. The cavity's terminating holes, labeled “3” in Fig. 2(a), are reduced in size and slightly displaced to increase the cavity Q-factor. Additionally, the radii of selected holes surrounding the cavity, labeled “2” in Fig.

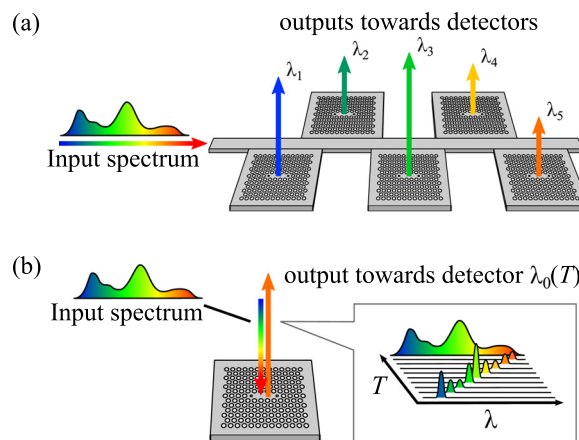


FIG. 1. Operating principle of a PhC cavity spectrometer using (a) an array of sequentially tuned cavities or (b) a single dynamically tunable cavity.

^{a)}Electronic mail: andreas.liapis@gmail.com

^{b)}Andreas C. Liapis and Boshen Gao contributed equally to this work.

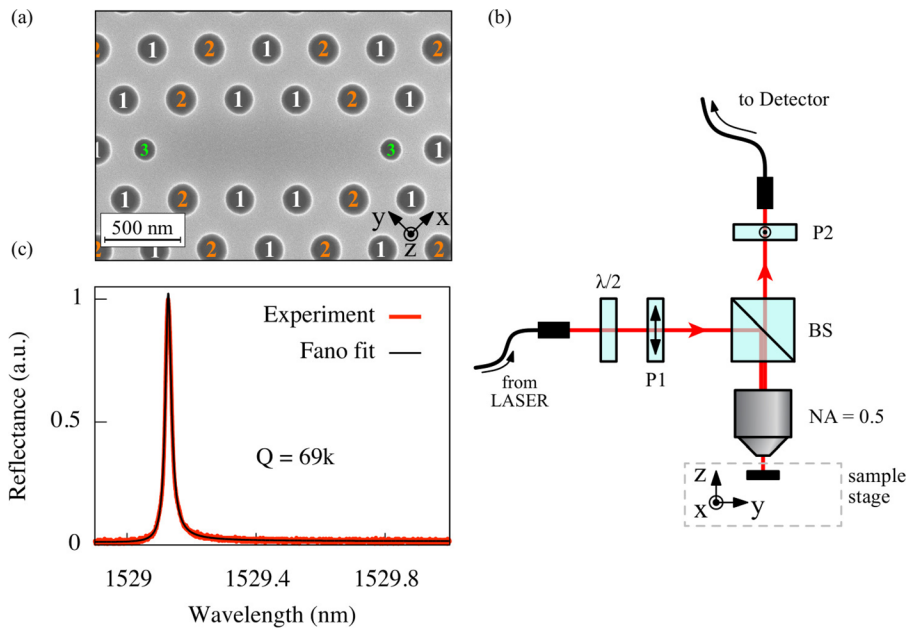


FIG. 2. (a) Scanning-electron micrograph of an L-3 PhC cavity optimized for vertical out-coupling. The holes are labeled according to their design radius. In this example, $r_1 = 89$ nm, $r_2 = 93$ nm, $r_3 = 62$ nm. Additionally, the holes labeled “3” are shifted outwards by 62 nm. (b) Schematic of the setup used to characterize PhC cavities via resonant scattering. P1 and P2: crossed polarizers, $\lambda/2$: half-wave plate, and BS: beam splitter. Note that the light incident on the PhC cavity is y-polarized and that only light that is x-polarized is being collected by the detector. (c) Measured resonance of a typical L-3 PhC cavity, displaying a Q of $\sim 69\,000$.

2(a), are slightly increased to modify the cavity’s far-field emission pattern and thus facilitate coupling in the out-of-plane direction. These PhC cavities were fabricated on commercial silicon-on-insulator wafers (SOITEC). The patterns were defined by electron-beam lithography on a positive-tone resist (ZEP 520) and transferred to the Si membrane by inductively coupled plasma etching using fluorine chemistry. After removal of the remaining resist, the buried oxide layer was undercut by wet chemical etching. A scanning-electron micrograph of one such cavity is shown in Fig. 2(a).

The fabricated cavities are characterized using resonant-scattering spectroscopy.¹⁵ In our experimental setup [Fig. 2(b)], the cavity axis is oriented at a 45° angle with respect to the polarization of the incident light, which is set by a half-wave plate and a polarizer. A second polarizer, oriented at a 90° angle with respect to the incident polarization, controls the polarization of light that reaches the detector. As a result of this arrangement, stray light reflected from the sample surface is suppressed, and only light that has scattered resonantly through the cavity is collected. The resonantly scattered intensity can then be fit with a Fano lineshape, from which we extract the resonance wavelength λ_0 and quality factor Q of the cavity.¹⁶ For a typical cavity, Q is approximately 69 000 [Fig. 2(c)].

To examine the dependence of the resonance wavelength on temperature, a heating element is attached to the sample mounting block. The temperature is monitored with a thermocouple and is stabilized using a proportional-integral-derivative feedback circuit. At each temperature point, we record the resonance wavelength λ_0 and coupling efficiency η , which is given by the ratio of scattered to incident optical power. A linear dependence of λ_0 on temperature is observed, with a slope of 0.07 nm/ $^\circ\text{C}$ (Fig. 3), which is consistent with what one would expect based on the temperature dependence of the refractive index of silicon.¹⁷ In the present demonstration, we limit ourselves to operating temperatures near room temperature in order to avoid thermal gradients across the sample holder, which would render the thermometry inaccurate. The useful tuning range is approximately 1.5 nm for a temperature

range of 20°C . The cavity Q -factor remains constant within 5% over this tuning range. In principle, this range could be extended by improved thermo-engineering design.

Once characterized, the cavity can be used to perform spectroscopy with a spectral resolution of 0.02 nm (or, equivalently, 3 GHz or 0.1 wavenumbers at a wavelength range near 1550 nm), which is comparable with the resolution of a tabletop spectrometer. The cavity is illuminated with the absorption spectrum we wish to measure, and the optical power scattered by the cavity is recorded as the temperature of the chip is tuned. In our experiment [Fig. 4(a)], the spectra are generated by passing laser light through commercial fiber-coupled gas cells (Wavelength References, Inc.) that contain different chemical species: a 5.5-cm long cell filled with acetylene to a pressure of 740 Torr and a 16.5-cm-long cell filled to a pressure of 150 Torr with hydrogen cyanide. In order to emulate broad-band illumination, we sweep the tunable laser over the wavelength range of

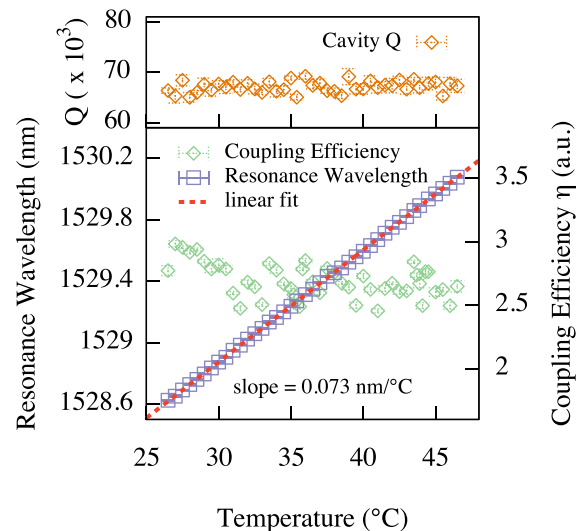


FIG. 3. Resonance wavelength, cavity Q , and coupling efficiency η as functions of temperature for an optimized L3 PhC cavity. A tuning range of 1.4 nm is demonstrated.

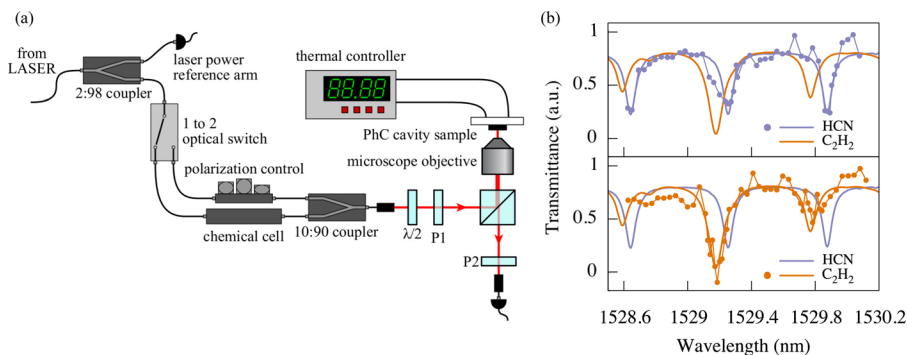


FIG. 4. (a) Schematic of the setup used for spectroscopic measurements. (b) Measured transmission spectra of the hydrogen cyanide (top) and acetylene (bottom) gas cells. The transmission of the two gas cells, measured using a tunable laser, is also shown (solid lines). Note that the spectral resolution is adequate to discriminate between the two gases.

1528.5–1530.2 nm, which covers lines P6–P8 of acetylene and R5–R7 of hydrogen cyanide and integrate the detected signal at each wavelength to obtain the total scattered optical power O . Fig. 4(b) shows the spectra measured using the PhC cavity, which are given by the ratio of the scattered optical power to the coupling efficiency O/η . Note that the alternating strength of the absorption lines seen in the spectrum of acetylene is due to the triple degeneracy of the antisymmetric rotational levels of this linear symmetric molecule, which is a result of the nuclear moments $I_H=1/2$ and $I_C=0$.¹⁸ Hydrogen cyanide, which is linear but not symmetric, does not display such an intensity alternation.

We see that the resolution of our cavity spectrometer is adequate to resolve neighboring absorption lines of acetylene and hydrogen cyanide. In principle, even better performance could be achieved by carefully optimizing the design of the PhC cavities to further increase their quality factor. Similar cavities were recently demonstrated with Q factors exceeding 1×10^6 .¹⁹ Note, however, that in our current setup, the spectral resolution is limited not only by the cavity Q but also by the stability of the thermal controller.

It is worth noting that by using a bus waveguide and multiple resonators, one could, in principle, perform parallel monitoring to decrease the data acquisition time. However, to construct a spectrometer of this type, we would need to fabricate a series of cavities whose resonances are equally spaced and span the target spectral range. The quality factor and resonance wavelength of PhC cavities can be chosen by appropriately tuning the design parameters, but not with arbitrary precision. Control is ultimately limited by the inherent imperfections of the fabrication process. Unavoidable imperfections in the resulting structure, such as sidewall roughness and lithographic inaccuracies, lead to variations in resonance frequency even among nominally identical cavities.²⁰ These variations become more pronounced for high-Q cavities, for which the uncertainty in resonance wavelength can be much larger than their resonance linewidth. As a result, unless these variations are corrected for, fabrication disorder limits the practical resolution of the spectrometer, as one is confined to using low-Q cavities only. Even though multiple techniques have been demonstrated,^{21–25} controllable post-fabrication tuning of individual PhC cavities remains a technical challenge.

In summary, we have demonstrated an implementation of a chip-scale spectrometer based on a dynamically tuned photonic crystal cavity. By utilizing a cavity optimized for vertical out-coupling, we avoid having to use a bus waveguide to

couple light into and out of the cavity and thus drastically decrease the footprint of the device. By monitoring the light reflected by this cavity as a function of temperature, we can extract spectral information with a resolution of 0.02 nm. Our device, therefore, overcomes the $1/L$ limit for the spectral resolution of dispersive spectrometers. A standard grating spectrometer would need a footprint with a scale size of at least 10 cm to achieve comparable resolution (0.1 cm^{-1}).

The authors would like to thank Antonio Badolato, Sebastian A. Schulz, David D. Smith, and Jerry Kuper for many fruitful discussions and acknowledge the assistance of Emily Conant in the early stages of the experiment. This work was supported by the U.S. Defense Threat Reduction Agency–Joint Science and Technology Office for Chemical and Biological Defense (Grant No. HDTRA1-10-1-0025), by the National Aeronautics and Space Administration (under Contract No. NNX15 CM47P), and by the Canada Excellence Research Chairs Program. Fabrication of the photonic crystal nanocavities was performed at the Cornell NanoScale Facility, a member of the National Nanotechnology Coordinated Infrastructure (NNCI), which is supported by the National Science Foundation (Grant No. ECCS-15420819).

¹M. K. Smit and C. Van Dam, *IEEE J. Sel. Top. Quantum Electron.* **2**, 236 (1996).

²Z. Shi and R. W. Boyd, *Opt. Express* **21**, 7793 (2013).

³B. Momeni, E. S. Hosseini, M. Askari, M. Soltani, and A. Adibi, *Opt. Commun.* **282**, 3168 (2009).

⁴B. Gao, Z. Shi, and R. W. Boyd, *Opt. Express* **23**, 6491 (2015).

⁵Z. Sun, K. McGreer, and J. Broughton, *IEEE Photonics Technol. Lett.* **10**, 90 (1998).

⁶B. B. Kyotoku, L. Chen, and M. Lipson, *Opt. Express* **18**, 102 (2010).

⁷C. Zhao, G. Li, E. Liu, Y. Gao, and X. Liu, *Appl. Phys. Lett.* **67**, 2448 (1995).

⁸S.-W. Wang, C. Xia, X. Chen, W. Lu, M. Li, H. Wang, W. Zheng, and T. Zhang, *Opt. Lett.* **32**, 632 (2007).

⁹N. K. Pervez, W. Cheng, Z. Jia, M. P. Cox, H. M. Edrees, and I. Kymissis, *Opt. Express* **18**, 8277 (2010).

¹⁰Z. Xia, A. A. Eftekhar, M. Soltani, B. Momeni, Q. Li, M. Chamanzar, S. Yegnanarayanan, and A. Adibi, *Opt. Express* **19**, 12356 (2011).

¹¹P. Deotare, L. Kogos, I. Bulu, and M. Loncar, *IEEE J. Sel. Top. Quantum Electron.* **19**, 3600210 (2013).

¹²X. Gan, N. K. Pervez, I. Kymissis, F. Hatami, and D. Englund, *Appl. Phys. Lett.* **100**, 231104 (2012).

¹³F. Meng, R.-J. Shiue, N. Wan, L. Li, J. Nie, N. C. Harris, E. H. Chen, T. Schröder, N. Pervez, I. Kymissis *et al.*, *Appl. Phys. Lett.* **105**, 051103 (2014).

¹⁴N.-V.-Q. Tran, S. Combré, and A. De Rossi, *Phys. Rev. B* **79**, 041101 (2009).

¹⁵M. W. McCutcheon, G. W. Rieger, I. W. Cheung, J. F. Young, D. Dalacu, S. Frédéric, P. J. Poole, G. C. Aers, and R. L. Williams, *Appl. Phys. Lett.* **87**, 221110 (2005).

- ¹⁶M. Galli, S. Portalupi, M. Belotti, L. Andreani, L. O'Faolain, and T. Krauss, *Appl. Phys. Lett.* **94**, 071101 (2009).
- ¹⁷B. Wild, R. Ferrini, R. Houdre, M. Mulot, S. Anand, and C. Smith, *Appl. Phys. Lett.* **84**, 846 (2004).
- ¹⁸G. Herzberg, *Molecular Spectra and Molecular Structure V. 2: Infrared and Raman Spectra of Polyatomic Molecules* (van Nostrand, 1945).
- ¹⁹Y. Lai, S. Pirota, G. Urbinati, D. Gerace, M. Minkov, V. Savona, A. Badolato, and M. Galli, *Appl. Phys. Lett.* **104**, 241101 (2014).
- ²⁰S. L. Portalupi, M. Galli, M. Belotti, L. C. Andreani, T. F. Krauss, and L. O'Faolain, *Phys. Rev. B* **84**, 045423 (2011).
- ²¹K. Hennessy, A. Badolato, A. Tamboli, P. Petroff, E. Hu, M. Atatüre, J. Dreiser, and A. Imamoglu, *Appl. Phys. Lett.* **87**, 021108 (2005).
- ²²A. Faraon, D. Englund, D. Bulla, B. Luther-Davies, B. J. Eggleton, N. Stoltz, P. Petroff, and J. Vučković, *Appl. Phys. Lett.* **92**, 043123 (2008).
- ²³K. Hennessy, C. Högerle, E. Hu, A. Badolato, and A. Imamoglu, *Appl. Phys. Lett.* **89**, 041118 (2006).
- ²⁴H. Lee, S. Kiravittaya, S. Kumar, J. Plumhof, L. Balet, L. Li, M. Francardi, A. Gerardino, A. Fiore, A. Rastelli *et al.*, *Appl. Phys. Lett.* **95**, 191109 (2009).
- ²⁵C. J. Chen, J. Zheng, T. Gu, J. F. McMillan, M. Yu, G.-Q. Lo, D.-L. Kwong, and C. W. Wong, *Opt. Express* **19**, 12480 (2011).